

# L-systems and partial differential equations\*

Mark Hammel and Przemyslaw Prusinkiewicz  
Department of Computer Science  
University of Calgary

## 1 Introduction

Interesting applications of parametric context-sensitive L-systems stem from their capability of expressing numerical solutions to initial value problems for partial differential equations. This capability was originally explored in the context of simulations performed using CELIA, the first software implementation of L-systems [2, 3, 9, 12], with the most general observations made in [10]. In this note, we present an approach to solving the initial value problem for PDEs with L-systems, using a parabolic (diffusion) equation as an example. We then apply this approach to solve a system of reaction-diffusion equations operating in a one-dimensional medium of constant size, as well as in an expanding medium. These solutions represent the evolution of the spatial distribution of the dependent variable(s) over time, and therefore lend themselves in a natural way to visualizations using extruded objects in space-time. In the examples considered, the visualizations lead to a realistic image of the shell of *Nautilus pompilius* with a pigmentation pattern, and to a graphical representation of the development of a filamentous bacteria *Anabaena catenula*.

## 2 Diffusion and decay

Let us consider the following equation:

$$\frac{\partial u}{\partial t} = -\nu u + D \frac{\partial^2 u}{\partial x^2}. \quad (1)$$

---

\*Adapted from: M. Hammel and P. Prusinkiewicz: Visualization of developmental processes by extrusion in space-time, Proceedings of Graphics Interface '96, pp. 246–258.

If  $u$  is interpreted as the concentration of a substance  $C$ , this equation represents the decay of  $C$  with time constant  $\nu$  and the diffusion of  $C$  along axis  $x$  with the diffusion coefficient  $D$  (for example, see [6]). Suppose that we want to solve this equation in the interval  $[a, b]$  for  $t \geq 0$ , assuming the boundary conditions  $u(a, t) = u_a, u(b, t) = u_b$ , and the initial conditions

$$u(x, 0) = u_a + (u_b - u_a) \frac{x - a}{b - a}. \quad (2)$$

Following the finite-difference method [19, Chapter 19], we approximate the derivatives in Equation (1) using values taken at equally spaced sampling points along both the  $x$  and  $t$  axes:

$$\begin{aligned} x_i &= x_0 + i\Delta x, & \text{where } i = 0, 1, \dots, m, \\ t_j &= t_0 + j\Delta t, & \text{where } j = 0, 1, 2, \dots \end{aligned} \quad (3)$$

Using notation  $u_i^j = u(x_i, t_j)$ , we obtain:

$$\frac{u_i^{j+1} - u_i^j}{\Delta t} = -\nu u_i^j + D \frac{u_{i+1}^j - 2u_i^j + u_{i-1}^j}{(\Delta x)^2}, \quad (4)$$

which leads to

$$u_i^{j+1} = u_i^j + \left( -\nu u_i^j + D \frac{u_{i+1}^j - 2u_i^j + u_{i-1}^j}{(\Delta x)^2} \right) \Delta t. \quad (5)$$

For any values of indices  $i$  and  $j$ , Equation (5) can be regarded as assigning a new value  $u_i^{j+1}$  to the variable  $u_i^j$ , taking into account the values  $u_{i+1}^j$  and  $u_{i-1}^j$  at the neighboring sampling points. Any sampling point along the axis  $x$  (except for the boundary points) is subject to a similar assignment, thus Equation (5) can be rewritten as the following context-sensitive L-system production:

$$M(u_l) < M(u) > M(u_r) \rightarrow M\left(u + (-\nu u + D \frac{u_l - 2u + u_r}{(\Delta x)^2}) \Delta t\right). \quad (6)$$

Notice that the L-system notation eliminates the need for index arithmetic. The subscripts in the formal parameter names  $u_l$ ,  $u$ , and  $u_r$  are not numbers, but mnemonic descriptors of the left and right neighbors. Similarly, indices are not needed to distinguish between the “old” and “new” values of variable  $u$  at any point in space, because the progress of time is implicit in the notion of a derivation step in an L-system.

To provide a framework for finite differencing expressed by production (6) a complete L-system solving Equation (1) must also:

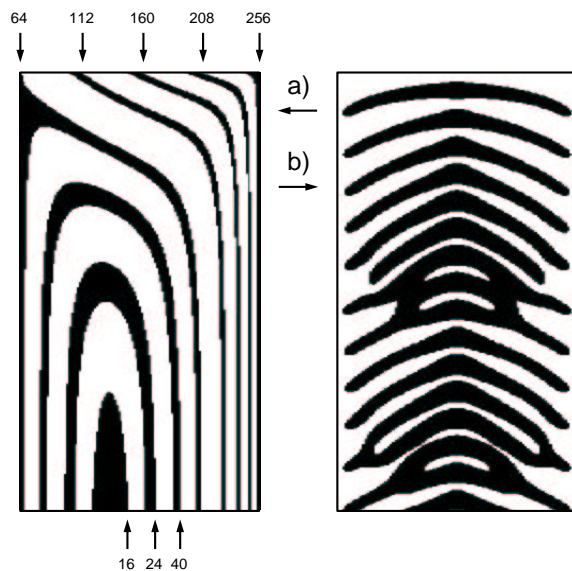


Figure 1: a) Visual representation of a solution to the PDE (1) obtained using an L-system based on production (6). Boundaries separating black and white regions indicate selected values of variable  $u$ . b) Visual representation of a solution to the PDE (7) obtained using an L-system based on production (10). White areas represent concentrations  $a < 0.15$ , and black areas represent concentrations  $a \geq 0.15$ . In both figures, time progresses from the top down.

- create a string of  $m$  modules  $M$  from the axiom,
- set the initial value of variable  $u$  in each module,
- maintain the boundary values of  $u$  in the first and the last modules  $M$  during the derivation process.

In addition, a graphical output must be associated with each module  $M$  if a visual representation of the solution is needed.

Figure 1a shows an extruded representation of the solution to PDE (1) obtained using an L-system in which each module  $M$  is shown as a line segment of unit length, with the color dependent on the value of variable  $u$ . The values of constants used in this simulation were:  $\nu = 0.01$ ,  $D = 5$ ,  $a = 0$ ,  $u_a = 64$ ,  $b = 128$ ,  $u_b = 256$ ,  $\Delta t = 1$ , and  $m = 128$ , yielding  $\Delta x = \frac{b-a}{m} = 1$ .

### 3 Reaction-diffusion

The described approach to solving partial differential equations using L-systems can easily be extended to systems of equations. In this case, a module  $M$  will have several parameters, each representing a different dependent variable. We will illustrate this technique by referring to reaction-diffusion models of the formation of pigmentation patterns in sea shells [7, 14, 15, 16, 17]<sup>1</sup>. The models recreate pattern formation in nature, which is characterized by Meinhardt as follows [15, p. vii]:

A mollusc can enlarge its shell only at the shell margin. In most cases, only at this margin are new elements of the pigmentation pattern added. Therefore, the shell pattern preserves a record in time of a process that took place in a narrow zone at the growing edge. A certain point on the shell represents a certain moment in its history. Like a time machine one can go into the past or the future just by turning the shell back and forth.

According to this description, a pigmentation pattern can be captured by simulating processes taking place at the growing edge and extruding this edge along an axis representing time. For example, the following system of differential equations was proposed by Meinhardt to model the formation of the pigmentation pattern on the shell of *Nautilus pompilius* [16] (see also [15, page 61]):

$$\begin{aligned}\frac{\partial a}{\partial t} &= a' - \mu a + D_a \frac{\partial^2 a}{\partial x^2}, \\ \frac{\partial s}{\partial t} &= \sigma(x) - a' - \nu s + D_s \frac{\partial^2 s}{\partial x^2},\end{aligned}\tag{7}$$

where

$$a' = \rho s \frac{a^2}{1 + \kappa a^2} + \rho_0,\tag{8}$$

and

$$\sigma(x) = \sigma_{min} + (\sigma_{max} - \sigma_{min}) \frac{2 \min\{x - x_{min}, x_{max} - x\}}{x_{max} - x_{min}}.\tag{9}$$

---

<sup>1</sup>The idea of modeling shell patterns using L-systems is not entirely new. Specifically, Baker and Herman generated pigmentation patterns similar to those found in *Oliva porphyria* [3] (see also [10, Chapter 18]) by applying L-systems to express a cellular automaton model proposed by Waddington and Cowe [21]. This approach preceded the formulation of the reaction-diffusion models of pigmentation, first reported in [14], and therefore did not expose the general possibility of expressing reaction-diffusion models using L-systems.

The variables  $a$  and  $b$  in Equation (7) describe concentrations of two chemical substances, called the *activator* and the *substrate*, which diffuse along the growing edge and react with each other. Equation (9) characterizes the production of the substrate  $\sigma(x)$  as a triangle-shaped function of the position of the sampling point  $x$  along the edge  $[x_{min}, x_{max}]$ .

To solve Equation (7) using an L-system, we discretize the growing edge and represent it as a string of modules  $M$ . The production that implements the finite difference method is:

$$\begin{aligned} M(a_l, s_l, \sigma_l) &< M(a, s, \sigma) > M(a_r, s_r, \sigma_r) \\ &\rightarrow M\left(a + (a' - \mu a + D_a \frac{a_l - 2a + a_r}{(\Delta x)^2})\Delta t, \right. \\ &\quad \left. s + (\sigma - a' - \nu s + D_s \frac{s_l - 2s + s_r}{(\Delta x)^2})\Delta t, \sigma\right). \end{aligned} \quad (10)$$

where  $a'$  is defined by Equation (8). As in the diffusion-decay example discussed in Section 2, the complete L-system for solving Equations (7) must also create the string of modules  $M$  and assign the initial and boundary values to the variables. This includes, in particular, the values of substrate production  $\sigma$ , which depend on the module position in the string (Equation 9).

A solution to Equation (7) in the interval

$$[x_{min}, x_{max}] = [0, 100] \quad (11)$$

with the initial conditions  $a(x, 0) = s(x, 0) = 0$  and boundary conditions  $a(0, t) = a(100, t) = s(0, t) = s(100, t) = 0$ , is visualized in Figure 1b. The following constants were used:  $\rho = 0.5, \kappa = 1, \rho_0 = 0.004, \mu = 0.1, D_a = 0.1, \nu = 0, D_s = 0.1, \sigma_{min} = 0.012, \sigma_{max} = 0.038, \Delta x = 1$ , and  $\Delta t = 1$ .

A realistic model of the *Nautilus* shell can be obtained assuming that the shell opening has the shape of a circle, growing exponentially from one derivation step to another, and that the axis of extrusion is coiled into a logarithmic spiral (see [7, 15] for details regarding the modeling of shell shape). Both phenomena can be easily expressed using an L-system, resulting in the model shown in Figure 2.

## 4 Reaction-diffusion in an expanding medium

The model of *Nautilus pompilius* extends the range of applications of L-system models to sea shells with pigmentation patterns. More generally,



Figure 2: Model of a *Nautilus pompilius* shell

it demonstrates that reaction-diffusion processes can be expressed using L-systems. However, the integration of reaction-diffusion processes and L-systems also leads to a wider class of models of morphogenesis, characterized by reaction-diffusion taking place in expanding media.

From a historical perspective, reaction-diffusion models were originally formulated under the simplifying assumption that the medium in which diffusion takes place does not grow [20]. This assumption dominated subsequent applications of the reaction-diffusion model. Exceptions include the consideration of edge growth in models of the pigmentation pattern of selected sea shells [15, 16], a model of stripe rearrangement during growth on the skin of the fish *Pomacanthus semicirculatus* [11], and a generic model of a growing filament that maintains a constant spacing between dividing and non-dividing cells [4]. In this section we present a related model of the development of the bacteria *Anabaena catenula*.

As described by Mitchison and Wilcox [18], the cells of *Anabaena* are organized into filaments which consist of sequences of *vegetative cells* separated by *heterocysts*. The vegetative cells divide into two cells of unequal length and, in some cases, differentiate into heterocysts which do not further

divide. Due to this differentiation, the organism maintains an approximately constant spacing between heterocysts: whenever the distance between two heterocysts becomes too large due to the division and elongation of vegetative cells, a new heterocyst emerges.

What mechanisms is responsible for the differentiation of heterocysts and the maintenance of constant spacing between them? Baker and Herman [2, 3] (see also [5, 9, 12] proposed the following model. The heterocysts fix atmospheric nitrogen and transform it into nitrogenous compounds. These compounds diffuse along the filament and are used by the vegetative cells. When the level of nitrogenous compounds drops below a threshold value, the cells that detect this reduced level differentiate into heterocysts.

Although the model of Baker and Herman is capable of reproducing the observed pattern of heterocyst spacing, it is very sensitive to parameter values. Small changes in these values easily result in filaments with pairs of heterocysts appearing almost simultaneously, close to each other. This is not surprising, considering the operation of the model. The gradient of the concentration of nitrogenous compounds may be too small near the middle of a sequence of vegetative cells to precisely define the point in which a new heterocyst should differentiate. Consequently, the threshold value may be reached almost simultaneously by several neighboring cells, resulting in the differentiation of two or more heterocysts close to each other.

The described model can be improved assuming that the prospective heterocysts compete until one “wins” and suppresses the differentiation of its neighbors. This “interactive” model was originally proposed by Wilcox *et al* [22]. We formalize it using the framework of the *activator-inhibitor* class of reaction-diffusion models [13]. In addition to the nitrogenous compounds that inhibit the differentiation, the cells are assumed to carry a hypothetical substance referred to as the activator. The concentration of the activator is the criterion that distinguishes the vegetative cells (low concentration) from the heterocysts (high concentration). The activator and inhibitor are antagonistic substances: the production of the activator is suppressed by the inhibitor unless the concentration of the inhibitor is low. In that case, production of the activator drastically increases through an autocatalytic process (an increased concentration of the activator promotes its own further production). High concentration of the activator also promotes the production of the inhibitor, which diffuses to the neighboring cells. This establishes a ground for competition in which activator-producing cells attempt to suppress production of the activator in the neighboring cells. For proper values of parameters that control this process, only individual, widely

spaced cells are able to maintain the high-activation state.

An L-system implementation of these mechanisms (a variant of the L-system from [8]) is given below:

$$\begin{aligned}
\omega &: M(0.5, 1, 200, \text{right})M(0.5, 1, 100, \text{right})M(0.5, 1, 100, \text{right}) \\
p_1 &: M(s_l, a_l, h_l, p_l) < M(s, a, h, p) > M(s_r, a_r, h_r, p_r) : \\
&\quad s < s_{max} \ \& \ a < a_{th} \rightarrow M(s', a', h', p) \\
p_2 &: M(s_l, a_l, h_l, p_l) < M(s, a, h, p) > M(s_r, a_r, h_r, p_r) : \\
&\quad s \geq s_{max} \ \& \ a < a_{th} \ \& \ p = \text{left} \rightarrow \\
&\quad M(ks', a', h', \text{left})M((1-k)s', a', h', \text{right}) \\
p_3 &: M(s_l, a_l, h_l, p_l) < M(s, a, h, p) > M(s_r, a_r, h_r, p_r) : \\
&\quad s \geq s_{max} \ \& \ a < a_{th} \ \& \ p = \text{right} \rightarrow \\
&\quad M((1-k)s', a', h', \text{left})M(ks', a', h', \text{right}) \\
p_4 &: M(s_l, a_l, h_l, p_l) < M(s, a, h, p) > M(s_r, a_r, h_r, p_r) : \\
&\quad a \geq a_{th} \rightarrow M(s, a', h', p)
\end{aligned} \tag{12}$$

where:

$$\begin{aligned}
s' &= s(1 + r\Delta t), \\
a' &= a + \left( \frac{\rho}{h} \left( \frac{a^2}{1 + \kappa a^2} + a_0 \right) - \mu a \right) \Delta t, \\
h' &= h + \left( \rho \left( \frac{a^2}{1 + \kappa a^2} + h_0 \right) - \nu h + D_h \frac{h_l + h_r - h}{sw} \right) \Delta t.
\end{aligned} \tag{13}$$

The cells are specified as modules  $M$ , where parameter  $s$  stands for cell length,  $a$  is the concentration of the activator,  $h$  is the concentration of the inhibitor, and  $p$  denotes polarity, which plays a role during cell division. All productions are context-sensitive to capture diffusion of the activator and inhibitor. It is assumed that the main barrier for the diffusion are cell walls of width  $w$ . Production  $p_1$  characterizes growth of vegetative cells ( $a < a_{th}$ ), controlled by the growth rate  $r$ . A cell that reaches the maximum length of  $s_{max}$  divides into two unequal daughter cells, with the lengths controlled by constant  $k < 0.5$ . The respective positions of the longer and shorter cells depends on the polarity  $p$  of the mother cell, as described by productions  $p_2$  and  $p_3$ . Increase of the concentration of the activator  $a$  to or above the threshold value  $a_{th}$  indicates the emergence of a heterocyst. According to production  $p_4$ , a heterocyst does not further elongate or divide. The equations for  $s'$ ,  $a'$ , and  $h'$  govern the exponential elongation of the cells and the activator-inhibitor interactions [13].

The operation of the model is illustrated in Figure 3. The vertical lines

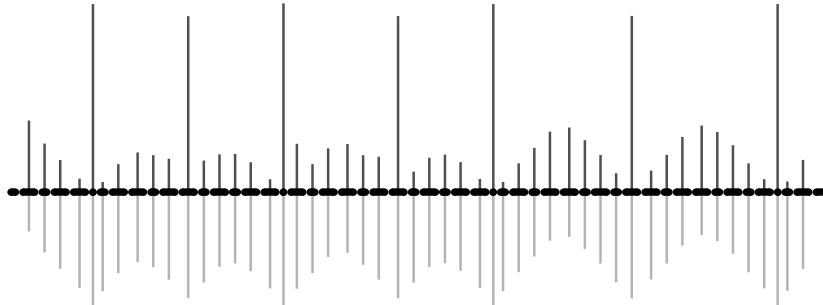


Figure 3: Fragment of a simulated filament of *Anabaena*. Vertical lines indicate the concentrations of the activator and inhibitor (above and below the cells, respectively). Notice the sharp peaks of the activator concentration that define the heterocysts, and high levels of the inhibitor concentration in the neighboring vegetative, which prevent their differentiation. The parameters used in the simulation were:  $\rho = 3$ ,  $\kappa = 0.001$ ,  $a_0 = 0.01$ ,  $\mu = 0.1$ ,  $h_0 = 0.001$ ,  $\nu = 0.45$ ,  $D_h = 0.004$ ,  $a_{th} = 1$ ,  $k = 0.38196$ ,  $s_{max} = 1$ ,  $r = 0.002$ , and  $w = 0.001$ .

indicate the concentrations of the activator (above the filament) and inhibitor (below the filament) associated with each cell.

It is interesting from the historical perspective that the interactive model of Wilcox *et al.* [22] and its subsequent L-system implementation [8] predicted the essential structure of the gene regulation network that controls the development of *Anabaena* filaments in nature [1]. The activator corresponds to the protein HetR, which plays a key role in the maintenance of the heterocyst state, whereas the inhibitor corresponds to the protein PatS (or a fragment of it), which diffuses across the filament and maintains the spacing between the heterocysts. The character of interactions captured by the simulation model is consistent with the postulated structure of the gene regulation network, in which HetR upregulates its own production as well as the production of PatS, whereas PatS downregulates production of HetR.

## References

- [1] D. G. Adams. Heterocyst formation in cyanobacteria. *Current Opinoin in Microbiology*, 3:618–624, 2000.

- [2] R. Baker and G. T. Herman. CELIA — a cellular linear iterative array simulator. In *Proceedings of the Fourth Conference on Applications of Simulation* (9–11 December 1970), pages 64–73, 1970.
- [3] R. Baker and G. T. Herman. Simulation of organisms using a developmental model, parts I and II. *International Journal of Bio-Medical Computing*, 3:201–215 and 251–267, 1972.
- [4] J.-P. Boon and A. Noullez. Development, growth, and form in living systems. In H. E. Stanley and N. Ostrowsky, editors, *On growth and form*, pages 174–183. Martinus Nijhoff Publ., Boston, 1986.
- [5] C. G. de Koster and A. Lindenmayer. Discrete and continuous models for heterocyst differentiation in growing filaments of blue-green bacteria. *Acta Biotheoretica*, 36:249–273, 1987.
- [6] L. Edelstein-Keshet. *Mathematical models in biology*. Random House, New York, 1988.
- [7] D. R. Fowler, H. Meinhardt, and P. Prusinkiewicz. Modeling seashells. Proceedings of SIGGRAPH '92 (Chicago, Illinois, July 26–31, 1992), in *Computer Graphics*, 26, 2 (July 1992), pages 379–387, ACM SIGGRAPH, New York, 1992.
- [8] M. Hammel and P. Prusinkiewicz. Visualization of developmental processes by extrusion in space-time. In *Proceedings of Graphics Interface '96*, pages 246–258, 1996.
- [9] G. T. Herman and G. Rozenberg. *Developmental systems and languages*. North-Holland, Amsterdam, 1975.
- [10] G. T. Herman and G. L. Schiff. Simulation of multi-gradient models of organisms in the context of L-systems. *Journal of Theoretical Biology*, 54:35–46, 1975.
- [11] S. Kondo and R. Asai. A reaction-diffusion wave on the skin of the marine angelfish *Pomacanthus*. *Nature*, 376:765–768, 31 August 1995.
- [12] A. Lindenmayer. Adding continuous components to L-systems. In G. Rozenberg and A. Salomaa, editors, *L Systems*, Lecture Notes in Computer Science 15, pages 53–68. Springer-Verlag, Berlin, 1974.

- [13] H. Meinhardt. *Models of biological pattern formation*. Academic Press, London, 1982.
- [14] H. Meinhardt. Models for positional signalling, the threefold subdivision of segments and the pigmentations pattern of molluscs. *Journal of Embryology and Experimental Morphology*, 83:289–311, 1984.
- [15] H. Meinhardt. *The algorithmic beauty of sea shells*. Springer-Verlag, Berlin, 1995.
- [16] H. Meinhardt and M. Klinger. A model for pattern formation on the shells of molluscs. *Journal of Theoretical Biology*, 126:63–89, 1987.
- [17] H. Meinhardt and M. Klinger. Pattern formation by coupled oscillations: The pigmentation patterns on the shells of molluscs. In *Lecture Notes in Biomathematics*, volume 71, pages 184–198. Springer-Verlag, Berlin, 1987.
- [18] G. J. Mitchison and M. Wilcox. Rules governing cell division in *Anabaena*. *Nature*, 239:110–111, 1972.
- [19] W. H. Press, S. A. Teukolsky, W. T. Vetterling, and B. P. Flannery. *Numerical recipes in C: The art of scientific computing. Second edition*. Cambridge University Press, Cambridge, 1992.
- [20] A. Turing. The chemical basis of morphogenesis. *Philosophical Transactions of the Royal Society of London B*, 237:37–72, 1952.
- [21] C. H. Waddington and J. Cowe. Computer simulations of a molluscan pigmentation pattern. *Journal of Theoretical Biology*, 25:219–225, 1969.
- [22] M. Wilcox, G. J. Mitchison, and R. J. Smith. Pattern formation in the blue-green alga, *Anabaena*. I. Basic mechanisms. *Journal of Cell Science*, 12:707–723, 1973.